Evanescent-Field Spectroscopy using Structured Optical Fibers: Detection of Charge-Transfer at the Porphyrin-Silica Interface

ARTICLE *in* JOURNAL OF THE AMERICAN CHEMICAL SOCIETY · MARCH 2009

Impact Factor: 12.11 · DOI: 10.1021/ja8081473 · Source: PubMed

J|A|C|S ARTICLES

Published on Web 02/09/2009

Evanescent-Field Spectroscopy using Structured Optical Fibers: Detection of Charge-Transfer at the Porphyrin-Silica Interface

Cicero Martelli,[†,‡] John Canning,[*,†,§] Jeffrey R. Reimers,[*,§] Maxine Sintic,[§] Danial Stocks,[§] Tony Khoury,[§] and Maxwell J. Crossley[*,§]

Contribution from the Interdisciplinary Photonics Laboratories, School of Chemistry, The University of Sydney NSW 2006; Department of Mechanical Engineering, Pontifica Universidade Catolica do Rio de Janeiro (PUC-Rio) Brazil; and the School of Chemistry, The University of Sydney, NSW 2006, Australia

Received October 20, 2008; E-mail: j.canning@usyd.edu.au; j.reimers@chem.usyd.edu.au; m.crossley@chem.usyd.edu.au

Abstract: The fabrication of porphyrin thin films derived from dichloro[5,10,15,20-tetra(heptyl)porphyrinato]tin(IV) [Cl−Sn(THP)-Cl] in the holes of photonic crystal fibers over 90 cm in length is described. Evanescent field spectroscopy (EFS) is used to investigate the interfacial properties of the films, with the high surface optical intensity and the long path length combining to produce significant absorption. By comparison with results obtained for similar films formed from Cl−Sn(THP)-Cl inside fused-silica cuvettes and on glass slides, the film is shown to be chemisorbed as a surface Si−O−Sn(THP)−X (X = Cl or OH) species. In addition to the usual porphyrin Q and Soret bands, new absorptions in the in-fiber films are observed by EFS at 445 nm and between 660−930 nm. The 660−930 nm band is interpreted as a porphyrin to silicon charge-transfer transition and postulated to arise following chemisorption at mechanical-strain induced defect sites on the silica surface. Such defect sites are caused by the optical fiber production process and are less prevalent on other glass surfaces. EFS within optical fibers therefore offers new ways for understanding interface phenomena such as surface adsorbates on glass. Such understanding will benefit all devices that exploit interface phenomena, both in optical fibers and other integrated waveguide forms. They may be directly exploited to create ultrasensitive molecular detectors and could yield novel photonic devices.

Introduction

In nature, porphyrins are responsible for important chemical (cellular respiration) and photochemical (photosynthesis) reactions. The design flexibility and low cost in manufacturing synthetic replicas with tailored functionalities make them important in many industrial areas (e.g., solar cells,[1] molecular recognition,[2] and electronic devices such as transistors[3]). Indeed, design flexibility, ease of fabrication, precise control over dimensionality, stability, and controllable π-electron delocalization make porphyrin thin-films likely candidates for industrial applications involving optics, electronics and/or optoelectronics. The incorporation of porphyrin thin films into optical waveguides promises a new generation of integrated optoelectronic devices. They potentially offer the possibility of combining electronic circuitry with optical functionality that modifies and controls a propagating mode within a waveguide.

To date, the incorporation of various materials into optical fibers has been demonstrated. For example, single-crystal semiconductor wires have been integrated into optical fibers,[4] presenting various intriguing possibilities for devices. Several gas sensing applications[5−7] have been reported which make use of photonic crystal fibers (PCF) and thick in-fiber layers have also been used as gas sensors (without the evanescent-field enhancement),[8,9] but instead relying on direct overlap within a bandgap structure. In more conventional fibers, evanescent field enhancement has been used to greatly increase sensitivity to make up for low interactions.[10,11] PCFs are structured waveguides that have channels with micron-sized diameters arranged in a periodic lattice around the core region running along the entire length of the fiber, possibly kilometers long.[12]

[†] Interdisciplinary Photonics Laboratories.
[‡] Department of Mechanical Engineering.
[§] School of Chemistry.

(1) Umezawa, Y.; Yamamura, T. *J. Electrochem. Soc.* **1979**, *126*, 705.
(2) Le Maux, P.; Bahri, H.; Simmoneaux, G. *J. Chem. Soc., Chem. Commun.* **1991**, 1350.
(3) Loppacher, C.; Guggisberg, M.; Pfeiffer, O.; Meyer, E.; Bammerlin, M.; Luthi, R.; Schlittler, R.; Gimzewski, J. K.; Tang, H.; Joachim, C. *Phys. Rev. Lett.* **2003**, *90*, 066107/1.
(4) Jackson, B. R.; Sazio, P. J. A.; Badding, J. V. *Adv. Mater.* **2008**, *20*, 1135.
(5) Hoo, Y. L.; Jin, W.; Ho, H. L.; Wang, D. N. *Opt. Eng.* **2002**, *41*, 8.
(6) Stewart, G.; Muhammad, F. A.; Culshaw, B. *Sens. Actuators B* **1993**, *11*, 521.
(7) Sudo, S.; Yokohama, I.; Yasaka, H.; Sakai, Y.; Ikegami, T. *IEEE Photonics Technol. Lett.* **1990**, *2*, 128.
(8) Jensen, J.; Hoiby, P.; Emiliyanov, G.; Bang, O.; Bjarklev, A. *Opt. Express* **2005**, *13*, 5883.
(9) Smolka, S.; Barth, M.; Benson, O. *Appl. Phys. Lett.* **2007**, *90*, 111101/1.
(10) Ghandehari, M.; Vimer, C. S. *NDT&E Int.* **2004**, *37*, 611.
(11) Schade, W.; Orghici, R.; Willer, U.; Waldvogel, S. *Proc. SPIE* **2008**, *7004*, 700431/1.
(12) Bjarklev, A.; Broeng, J.; Sanchez Bjarklev, A. *Photonic Crystal Fibres*; Kluwer Academic Publishers: Dordrecht, 2003.

PCFs are a class of structured optical fibers that includes phase adjusted structures (Fresnel fibers)[13] and omnidirectional fibers.[14] In contrast to conventional fibers, much greater optical field overlap with the glass-channel interfaces can take place, up to orders of magnitude compared to conventional sensors where access to the evanescent field is done through the use of, for example, higher order modes within multimode optical fibers or through etching the cladding less to access the core. Since propagation remains in the core, extremely long interface interactions are possible compared to direct overlap spectroscopy obtained using bandgap fibers.

Our aim in this work is to line the surface of fiber channels with a monolayer, leaving them open to and still able to support the flow of liquids and gases. To do this, we exploit both the ability of quasi-planar porphyrin systems to form self-assembled monolayers on surfaces[15] and the known chemistry of dichlorotin(IV) porphyrins to react with hydroxyls,[16] in this case surface silanol groups, to generate a chemisorbed monolayer. The position of the holes in close proximity to the core allows a range of novel functions to be incorporated that are not possible in an all-solid conventional optical fiber.

In this study, the technique of evanescent-field spectroscopy (EFS) is applied to the study of chemisorptions on the inner holes of photonic fibers. The evanescent field of the propagating mode makes an ideal spectroscopic probe to study the chemistry and photophysical properties of species that lie on the surfaces of the holes. Here, the chemisorption of porphyrin thin films, most likely at submonolayer coverage on the surface of the holes, enable both study of the interface and the development of robust techniques for modulating the optical properties of the fiber.

Adsorbate Molecule Design Considerations. As shown in Figure 1, the diameters of the holes that run continuously for the entire length of the photonic crystal fiber used in this work vary from 2.5 μm (inner ring of holes) to >4 μm (outer ring of holes). This gives a radius of curvature that allows the surface to be, for all intent and purposes, planar with respect to the molecules. Most of the optical field interacts with the innermost ring.

The chromophore molecules are desired to chemisorb to the surface forming regular monolayers. We choose to attach a metalloporphyrin in which the metal ion has octahedral coordination by forming a bond between the metal ion and an O atom of a surface silanol. It is clear that the metalloporphyrin itself should not have meso-substitutents such as phenyl or other aryl groups that project orthogonally to the macrocyclic plane as this will sterically impede the coordinated metal ion from bonding to the surface. Axial O−Sn bonds can be created by replacement of an axial ligand of dihydroxotin(IV) porphyrins or the corresponding dichlorotin(IV) porphyrins.[16] The reaction of tris(*tert*-butyl)silanol with dihydroxotin(IV) 5,10,15,20-tetraphenylporphyrin HO-Sn(TPP)-OH to give $(^t\mathrm{BuO})_3\mathrm{Si}-\mathrm{O}-\mathrm{Sn(TPP)}-\mathrm{O}-\mathrm{Si}(\mathrm{O}^t\mathrm{Bu})_3$ has been demonstrated but the conversion was slow and required azeotropic removal of the resultant water by using refluxing toluene as solvent under a Dean−Stark trap to drive the reaction; similarly, in chloroform at room temperature the reaction required 4 days to go to completion.[17] The former reaction conditions were used to react HO-Sn(TPP)-OH with a glass bead surface but this resulted in the formation of a coating up to a few microns thick, presumably some form of multilayer through hydrogen bonding networks involving the intermolecular interactions of hydroxo ligands (physisorption) or through additional dehydrations leading to formation of μ-oxo [eg., $(\mathrm{surfaceSi-O-SnTPP-O-(SnTPP-O)}_n\mathrm{-H}$] species under the Dean−Stark conditions.[17] The reaction of alcohols and carboxylic acids with dichlorotin(IV) porphyrins to give the corresponding di(alkyoxo)tin(IV) and dicarboxylatotin(IV) porphyrins occurs at room temperature and is much more rapid than similar reactions on the dihydroxotin(IV) porphyrins. Dichlorotin(IV) porphyrins were expected to share the same reaction with the surface silanol groups[18] as do the dihydroxotin(IV) porphyrins; however, they are expected to react readily at room temperature. Furthermore, retaining one chloro ligand on the top face would prevent multilayer formation through some sort of oligomerization involving hydrogen-bonding or μ-oxo bonds.

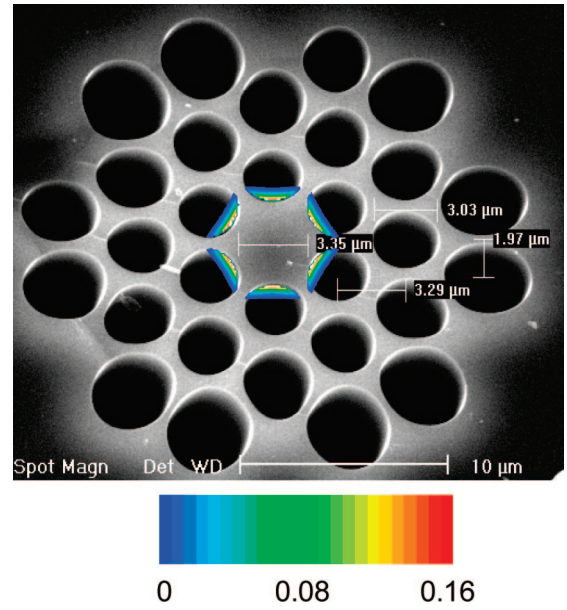

Figure 1. Scanning electron microscope (SEM) image of the fiber cross-section used in the experiments and the calculated evanescent field within the holes; the field intensity is normalized to the peak intensity of the fiber fundamental mode at 480 nm confined in the core region (not represented in the image).

From the considerations described above, the porphyrin molecule chosen to fulfill the requirements of pseudoplanarity and ready reactivity with the silanol group is dichloro[5,10,15,20-tetra(heptyl)porphyrinato]tin(IV) (Figure 2a). The expected reaction is shown in Scheme 1.

We place the alkyl chains at the meso positions of the porphyrin to promote self-assembly of the molecules. While scanning tunneling microscopy (STM) measurements have confirmed such alignment and packing in porphyrin monolayers physisorbed on Au(111) surfaces,[15] similar measurements on silica surfaces are somewhat challenging due to the low

(13) Canning, J. *Opt. Commun.* **2002**, *207*, 35.
(14) Fink, Y.; Winn, J. N.; Fan, S.; Chen, C.; Michel, J.; Joannopoulos, J. D.; Thomas, E. L. *Science* **1998**, *282*, 1679.
(15) Hulsken, B.; van Hameron, R.; Gerritsen, J. W.; Khoury, T.; Thordarson, P.; Crossley, M. J.; Rowan, A. E.; Nolte, R. J. M.; Elemans, J. A. A. W.; Speller, S. *Nature Nanotechnol.* **2007**, *2*, 285.
(16) Arnold, D. P.; Blok, J. *Coord. Chem. Rev.* **2004**, *248*, 299.
(17) Langford, S. J.; Latter, M. J.; Beckmann, J. *Inorg. Chem. Commun.* **2005**, *8*, 920.
(18) *Proceedings of the NATO Advanced Study Institute on Defects in SiO_2 and Related Dielectrics: Science and Technology, held 8−20 April 2000, in Erice, Italy*; Pacchioni, G.; Skuja, L.; Griscom, D. L., Eds.; Kluwer Academic Publishers: Dordrecht, 2000.

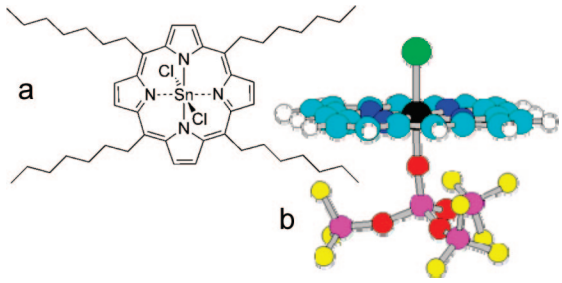

Figure 2. (a) Structure of dichloro[5,10,15,20-tetra(heptyl)porphyrinato-]tin(IV), and (b) optimized structure of a porphyrin-silica model cluster Cl−Sn(P)−O−Si(OSiF$_3$)$_3$ where P is the porphyrin ring system (cyan, C; white, H; black, Sn; green, Cl; red, O; purple, Si; yellow, F).

Scheme 1

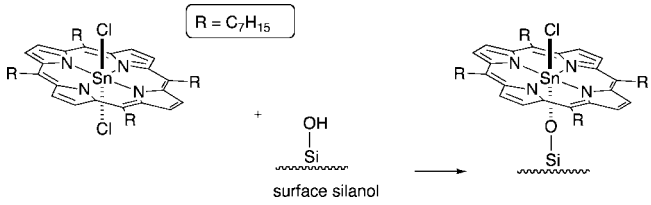

conductivity and lack of atomic organization of amorphous silica. Nevertheless, a cofacial arrangement of chemisorbed reactant to the silica surface is expected, and a model cluster displaying the proposed attachment mechanism is shown in Figure 2b. The length of the meso alkyl chains significantly influences both solubility and self-assembly properties; we choose a short length of 7 CH_n units in this initial study so as to enhance solubility in *N*,*N*-dimethyl formamide (DMF) and to minimize interchain interactions.

Results

Our experimental results indicate that a robust and stable film does indeed adhere to the surface of the holes in the optical fiber. We discuss in detail the preparation of the fiber, the nature of the dry film initially produced, and the nature of a modified film produced by subsequent washing with DMF and then with dichloromethane (DCM). First, however, we consider thin films chemisorbed to flat glass surfaces, analogously washing the film with DMF and DCM as well as with chloroform, tetrahydrofuran (THF), acetone, and the weak base K_2CO_3 in 5:1 THF:H_2O solution. Such films are more amenable to standard chemical analysis techniques such as X-ray photoelectron spectroscopy (XPS) than are films inside optical fibers.

Solution Spectrum of Porphyrin. Figure 3 shows the spectrum of dichloro[5,10,15,20-tetra(heptyl)porphyrinato]tin(IV) in DMF solution; this is dominated by the intense Soret band at 426 nm but weak Q bands at 569 and 609 nm are also observed (Table 1). The oscillator strength of the Soret band is measured to be 1.72 and this value is subsequently used to estimate the coverage of thin films.

Films on Flat Glass Surfaces. Shown in Figure 4 is the transmission absorption spectrum of a thick solid formed by the evaporation of a chloroform solution of dichloro[5,10,15,20-tetra(heptyl)porphyrinato]tin(IV) inside a fused-silica UV cuvette. The solid in the region of the light path appeared somewhat uniform to the eye but darker spots of ∼1 mm diameter appear at ∼5 mm spacing throughout; however, the film was very thick along the edges and near the corners of the cuvette. As summarized in Table 1, compared to the liquid

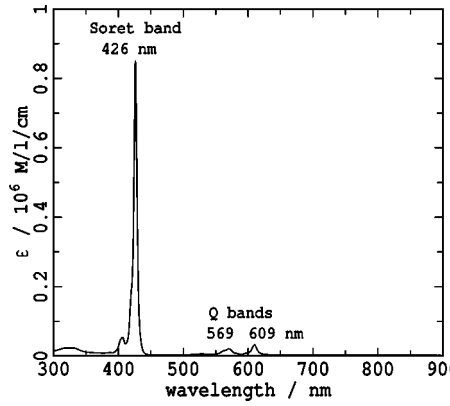

Figure 3. Molar extinction coefficient ε for dichloro[5,10,15,20-tetra(heptyl)porphyrinato]tin(IV) in DMF solution.

sample (Figure 3), the spectrum of the solid shows sharp Q bands red-shifted by ∼15 nm, while the Soret band is broadened to cover the whole 400−450 nm spectral region (note that there is no discernible absorption of the solid at energies below 650 nm). Assuming that the oscillator strength of the Soret band is not modified by the interporphyrin interactions and an approximate molecular area of 1.5 nm^2 in a supposed flat-lying conformation, the average film thickness in the light path is estimated to be 54 molecules.

The solid was then washed thoroughly using a sequence of solvents with the spectrum obtained after each wash displayed in Figure 4. First, the solid was washed using DMF and the spectra recorded while a thin film of the solvent remained covering the cuvette walls. The porphyrin Soret band is distinct and appears similar to that in the solution spectrum shown in Figure 3 with a sharp maximum near 423−425 nm; the Q bands are very weak but can also be discerned in the spectrum in the region of 570 and 610 nm, similar to the values observed in solution. From the integrated intensity, the surface density is determined to be 0.057 molecules nm^{-2} so that the coverage is ∼0.09 of that for a close-packed flat-lying monolayer. Following this, the DMF was evaporated by blowing with nitrogen gas and the spectrum recorded (Figure 4). Desolvation has only a minor effect, but weak bands at 407, 465, and 510 nm are discernible, indicating that a small amount of the previously characterized solid formed during the evaporation; as a result, the apparent coverage of the major species reduces only slightly to ∼0.08. However, when a fluorescence cuvette is used so as to allow the transmission to be measured through the walls orthogonal to the surface on which the original solid was deposited, a nearly identical spectrum is measured. This indicates that flooding the cuvette with DMF not only dissolved the nonattached porphyrin solid but also induced attachment of the porphyrin to all accessible silica. As the light path in the dried cuvette crosses two surfaces, the coverage per surface is thus ∼0.04 of a monolayer (surface density of 0.025 nm^{-2}).

Washing this dried film with DCM and redrying resulted in only the removal of the remnant solid; subsequent wash/dry cycles using acetone and THF had no effect on the film and the apparent coverage per surface remains at 0.04 of a monolayer. This indicates that the remnant film is strongly attached to the silica surface. Finally, the film was soaked in a solution of K_2CO_3 in 5:1 THF:H_2O for 24 h and then washed with THF and dried. The resulting spectrum, shown in Figure 4, is an order of magnitude weaker, and a final was with DCM removes all trace of the film. As K_2CO_3 in 5:1 THF:H_2O is a

Table 1. Absorption Maxima and the Full-Width at Half Maximum, FWHM, for [5,10,15,20-Tetra(heptyl)porphyrinato]tin(IV) Bands Observed in Bulk Solution As Well As in Films Located Either in Cuvette, On Silica or Soda-Glass Slides, Or in Fiber, Either with Solvent or Dry

	Soret fwhm nm	Soret band nm	new band nm	Q-band nm		new band nm
bulk solution (DMF)	5	426		569	609	
in cuvette (solid, dry)	120	407, 465(sh), 510(sh)		583	624	
in cuvette (thin film, dry)	10	423−425		∼570	∼610	
on silica slide (solid, dry)	125	410, 464(sh), 504(sh)		584	625	
on silica slide (thin film, dry)	11	424				
on glass slide (thin film, dry)	10	422		∼570	∼610	
in fiber (thin film, dry)	25	416		561	602	
in fiber (dried film + DMF)	13	420	445	559	599	660−930
in fiber (after DCM wash, dry)	13	419				

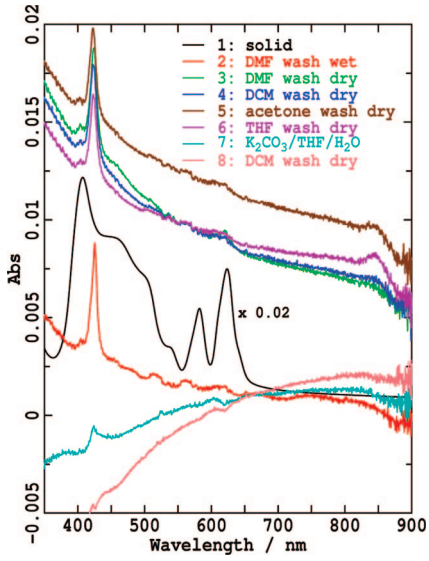

Figure 4. Transmission absorption spectra of a solid [5,10,15,20-tetra-(heptyl)porphyrinato]tin(IV) layer inside a fused-silica cuvette (using a similar cuvette as reference) obtained during sequential wash and/or dry cycles using DMF, DCM, acetone, THF, and the weak base K_2CO_3 in 5:1 THF:H_2O.

very mild base that reacts specifically with oxygen to tin(IV)porphyrin bonds,[19] this result supports the chemisorption mechanism outlined in Scheme 1. The low coverage attained indicates that only a small fraction of the silica surface contains sites suitable for reaction.

Sample films of the porphyrin on both very flat (<10 nm roughness) soda glass slides and highly polished high-purity fused-silica slides were prepared and found by optical absorption to have similar coverage (∼0.05 of a monolayer) and similar spectra (Table 1) to the films previously described formed inside the fused-silica cuvette. The slides were analyzed by XPS for their relative chlorine and tin content and all gave similar results. Substantial signals were observed for tin, indicating that it is indeed a tin(IV) porphyrin that attaches to the surface. No signal was observed for chlorine, however, indicating that both chlorines from the dichloro[5,10,15,20-tetra(heptyl)porphyrinato]tin(IV) reactant have been lost or replaced. For calibration purposes, samples of the dichloro porphyrin and its dihydroxo analogue were prepared physisorbed to highly ordered pyrolitic graphite (HOPG) surfaces, with the dichloro compound showing a significant chlorine to tin signal ratio. Hence, these results are consistent with the postulated reaction mechanism (2) but indicate that additional processes must also have occurred.

(19) Crossley, M. J.; Thordarson, P.; Wu, R. A. S. *J. Chem. Soc., Perkin Trans. 1* **2001**, 2294.

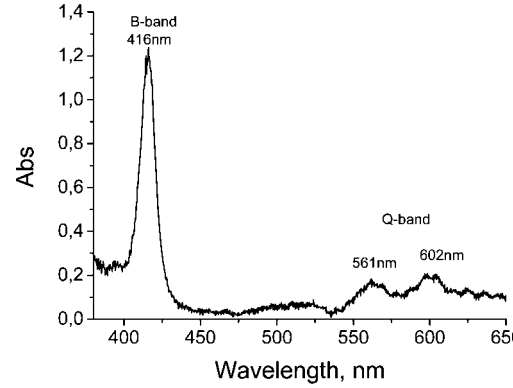

Figure 5. Absorption spectrum of a 90 cm long fiber sample coated with a porphyrin thin-film in the presence of air.

Optical Fiber Construction. Figure 1 shows a cross section of the fiber (fabricated from stacking a series of capillaries, fusing these and subsequently drawing) used and the simulated evanescent field of the fundamental mode overlapping with the holes. As the refractive index of the fiber increases significantly when solvent is present in the core, the actual magnitude of the evanescent-field strength can vary considerably. The radius is sufficiently large so that for all intents and purposes the molecules see a flat surface. These types of waveguides are tailored by distributing the holes as desired during the stacking process, which permits a wide scope of novelty in hybrid optoelectronic organic and inorganic technologies, i.e., "opto-organo" circuits.

Preparation and characterization of initial dry film. A solution of the porphyrin dichloro[5,10,15,20-tetra(heptyl)porphyrinato]tin(IV) in DMF was pumped through the fiber followed by flushing with pure solvent and then heating and purging with dry nitrogen gas. The absorption spectrum of the resulting fiber sample is shown in Figure 5. While no trace of DMF is observed in the near-IR region (not shown in the plot), both the B (Soret) and Q porphyrin absorption bands are observed, indicating that the porphyrin remains inside of the fiber channels. By analogy with the results demonstrated for this porphyrin on flat glass surfaces, the remaining material is identified as a chemisorbed thin film. Fiber cut-back measurements of all absorption bands indicate a standard Beer−Lambert dependency with length, consistent with a uniform film along the fiber length.

The most noticeable features of the in-fiber absorption porphyrin spectrum are the observed blue shifts of ∼10 nm of both the Soret and Q-band systems, and the unusually large full-width at half-maximum (fwhm) of the Soret band of 25 nm, as detailed in Table 1. These features were not detected for the porphyrin films in the cuvette or on the glass slides.

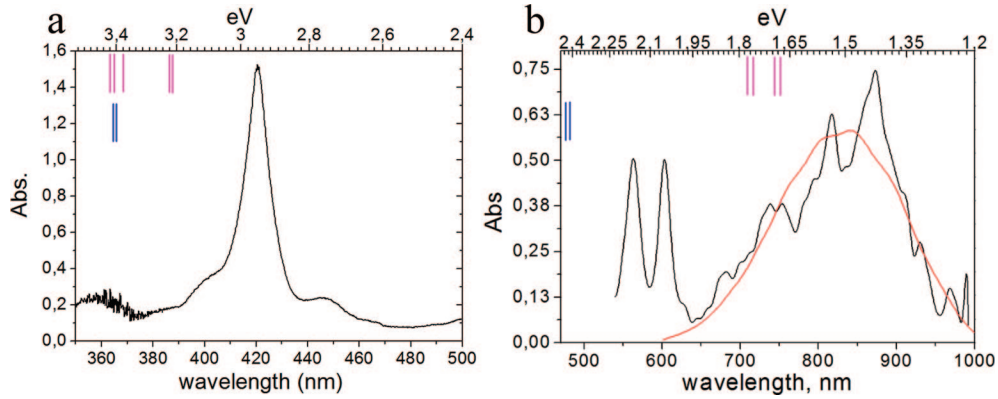

Figure 6. Absorption measurement of the fiber samples containing the porphyrin thin-films deposited on the surfaces of its holes in DMF: (a) the absorption spectrum of fiber sample (length = 25 cm) showing the Soret band (420 nm) and the new band at 445 nm; (b) absorption spectrum of fiber sample (length = 50 cm, absorption rescaled to 25 cm) where the Q-band (559 and 599 nm) and the new near-IR band (660−930) nm can be observed. Shown in red is a typical charge-transfer band contour (see text). TDDFT calculated energies for the two considered porphyrin-silica chemisorption products are represented by the blue (regular silica surface−SiO_4) and pink (oxygen deficient surface defect−SiO_3) lines.

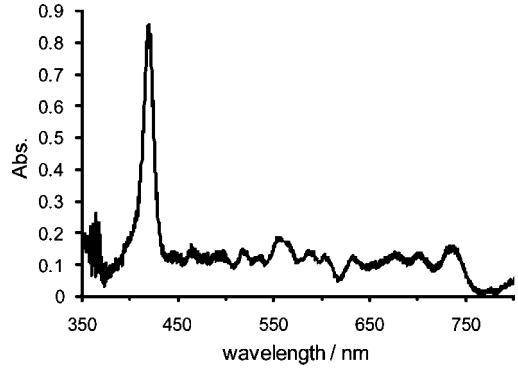

Figure 7. Absorption measurement of the fiber samples (length = 25 cm) containing the porphyrin thin-films deposited on the surfaces of its holes in DMF fiber after washing with DCM, showing the Soret band at 419 nm.

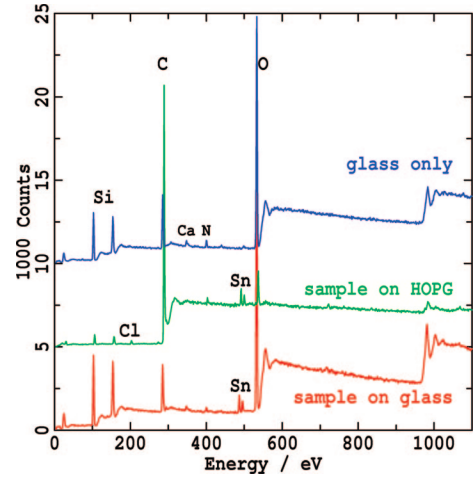

Figure 8. XPS spectra of dihydroxo[tetra(heptyl)porphyrinato]tin(IV) on fused-silica glass and on HOPG, compared to the spectrum of the blank fused-silica glass. Evidence for significant contamination of the HOPG by silicates and of the glass by organics is evident, but no contamination by Sn or Cl is found, indicating that the relative magnitudes of these signals indicates aspects of the chemical nature of the adsorbate layers.

New Absorption Bands Appear upon Resolvation. When DMF solvent is added to the previously dried fibers, the major features of the absorption are preserved but new absorption bands are also observed. Figure 6 shows the absorption spectra of such a fiber in the (a) visible and (b) near-infrared regions: a sharp porphyrin-like band appears at 445 nm adjacent to the Soret band, as well as a broad feature in the near-IR extending from 660−930 nm. Similar additional new features were not observed following resolvation of analogously washed thin films inside the fused-silica cuvette or on the soda-glass slides. The Soret band sharpens and red shifts on solvation, moving from 416 nm center, 25 nm fwhm to 420 nm center, 13 nm fwhm (Table 1). While distinct structure is observed within the 660−930 nm broad absorption band, its shape mimics the observed absorption characteristics of the fiber and is therefore not indicative of actual quantitative molecular-absorption band structure.

New Bands May Be Irreversibly Removed. Washing the optical fiber with DCM significantly reduced the absorption intensity (Figure 7), leaving behind a species that has the typical porphyrin absorption bands but *does not* display the additional bands. Replacement of the DCM with DMF inside the fiber does not recover the new bands, indicating that the DCM wash irreversibly removed the absorbing species. A sharp Soret band centered at 419 nm with a fwhm of 13 nm is observed, similar to that found earlier after resolvation by DMF. Thus, the original film is shown to contain two components, one with properties akin to the films produced inside the fused-silica cuvette or on the glass slide that is strongly attached to the surface, and one that is more weakly attached with a sharp but solvent sensitive Soret band that also displays new absorption bands.

Discussion

On the walls of high-purity fused-silica cuvettes and fused-silica slides, as well as on the surface of ultraflat (<10 nm surface roughness) soda glass slides, dichloro[5,10,15,20-tetra(heptyl)porphyrinato]tin(IV) was shown to chemisorb with a low coverage of the order of 0.025 of a monolayer, and a film with very similar properties was also produced inside the optical fibers. XPS measurements, shown in Figure 8, indicate that the adsorbate contains tin while spectroscopic measurements show that a porphyrin very similar to the reactant is bound; hence it is clear that the adsorbate is a Sn(IV) porphyrin. All trace of chlorine is lost, however, and so as Sn(IV) porphyrins are all 6-coordinate, it is clear that both original ligands have been replaced. This is consistent with the proposed chemisorptions reaction (Scheme 1) in which one chlorine is lost through reaction with a surface silanol group to eliminate HCl. The XPS

experiments provide no evidence to suggest that the sixth ligand is anything other than oxygen and hence it is likely that the product from Scheme 1 undergoes a subsequent reaction

$$\text{surfaceSi}-\text{O}-\text{Sn(THP)}-\text{Cl} + \text{H}_2\text{O} \rightarrow \text{surfaceSi}-\text{O}-\text{Sn(THP)}-\text{OH} + \text{HCl}$$

where THP represents the 5,10,15,20-tetraheptylporphyrin ring system; the reactant water could come from either atmospheric exposure of the adsorbate or from trace impurities in the original DMF solvent. In support of this argument, mixed chloro(hydroxy)tin(IV) porphyrins in solution are known to be activated toward this elimination reaction compared to their dichloro analogues.[16] It is noted, however, that while the UV spectrum of the dihydroxo analogue in solution (see Experimental Section) shows a blue shift of 3 nm compared to the dichloro compound, in agreement with the changes observed on chemisorptions (Table 1), other effects of adsorption have not been quantified.

Inside the fiber, absorption measurements indicate that a second porphyrin species also attaches to the surface that can be washed away using DCM. While porphyrin solids can show Soret bands with the properties similar to those of the new species,[20] from the observed spectra it is clear that this species is not just simply a deposited solid of the porphyrin. Alternatively, an initial conclusion might be that the observed Soret band could arise from a surface-directed porphyrin dimerization process since typical Soret red shifts[21,22] for porphyrin sheets are of order 8 to 13 nm with an additional red shift of 4 nm for applicable π-stacked layers; this is consistent with the observed shifts.[21] Unfortunately, this type of chemical model cannot account for the observed new absorption band in the 660−930 nm region of the spectrum, and thus there exists no realistic proposal for the nature of all of the new bands that does not involve an active role for the surface.

When dried, the alternate chemisorbate displays the spectrum of a simple single porphyrin, indicating that chemical variations associated with the binding must occur within the surface rather than directly involving the surface to chromophore bond. Also, the observed, unusually broad, new band in the 660−930 nm region has the typical appearance of a charge-transfer (CT) transition,[23,24] possessing a realistic width for such a band. Further still, the observed band is only seen in the presence of solvent, a rare property that is characteristic of CT transitions. It is hence most likely that the two species observed in the fibers differ by their site of chemisorptions onto the silica surface, with the fiber-only site being one that supports CT bands.

Pursuing this line of argument, the surface of silica is rough and presents many types of reactive sites to which the dichlorotin(IV) porphyrins could bind. For the chemisorbate component that formed on all of the media studied, the observed coverage of ~0.025 of a monolayer (in cuvettes and on slides) indicates that the porphyrin is somewhat selective in terms of its reactivity to the surface. To explain differences in results between fiber and bulk samples, it is worth noting that a most significant difference between the optical fiber and the cuvette/glass slide arises from their fabrication. Optical fibers are produced under large mechanical forces while being rapidly quenched during fiber drawing. Structured optical fibers, in particular are produced under conditions where through Poisson's ratio there are huge compressive forces on the air holes which are pressurized during drawing to keep them open; upon quenching some of the large mechanical strains are expected to be frozen into the glass. Previous work has shown that on mechanically strained glass, free-radical defect sites account for up to 10% of the surface.[18] The most common form of free-radical sites is the one in which a silicon bond to oxygen is absent so that the silicon coordination number is three instead of four, thus forming a surface free radical.[18] It is probable that the inner surface of the air channels of the final optical fiber may have a significant number of analogous surface free radicals. Electronic transitions involving both the porphyrin and such a surface free-radical would thus be of a CT nature; the observed experimental results can therefore be accounted by in-fiber weakly chemisorbed species associated with such free-radical chemisorption sites. Owing to the less sterically hindered nature of the porphyrin to rear-side attack at the free-radical site, as well as to the intrinsic reactivity of the site itself, a variety of mechanisms are possible for the cleavage of the porphyrin by DCM. For example, chlorinated hydrocarbon solvents such as CCl_4 and DCM react with silanol surface sites at elevated temperatures[25,26] as well as with molecular silyl radicals at room temperature.[27,28] Hence, it is feasible that either DCM itself, or a trace contaminate such as CCl_4, could attach a silyl radical on the fiber surface; alternatively, trace HCl in the DCM could attack the tin porphyrin.

To test the feasibility of the radical-chemisorption-site model, the band structure of a typical CT involving a porphyrin and such a surface site has been simulated and the results are compared to the observed band contour in Figure 6b. Electron−phonon coupling in two modes, one describing the effects of oxidation of the porphyrin ring and the other the effects of reduction on the Si−O bonds, are included. The qualitative match with the observed absorption suggests that a CT model can readily account for the observed new absorption feature. No model involving only porphyrin spectroscopic transitions can similarly account for these features.

Time-dependent density-functional theory (TD-DFT) calculations have also been performed to estimate the spectrum of chemisorbates at both regular (four coordinate tetrahedral) and defect (three coordinate tetrahedral radical) sites. The predicted transitions are indicated in Figure 6, parts a (Soret region) and b (Q bands and near-IR region). While some significant disparities in the absolute values of the calculated absorption energies are apparent, the major features of the washed-out absorptions are reproduced. This includes both the appearance of a shoulder to the red of the Soret band and the appearance of a broad solvent dependent near-IR CT band. The calculations also predict substantial lowering of the Q-band absorption frequencies but as these bands are expected to be much less

(20) Ishii, K.; Kayobayashi, N. In *The Porphyrin Handbook*; Kadish, K. M., Smith, K. M., Guiland, R., Eds.; Academic Press: San Diego, 2003; Vol. 16; pp 1.
(21) Komatsu, T.; Moritake, M.; Nakagawa, A.; Tsuchida, E. *Chem.−Eur. J.* **2002**, *8*, 5469.
(22) Tsuchida, E.; Komatsu, T.; Arai, K.; Yamada, K.; Nishide, H.; Fuhrhop, J.-H. *Langmuir* **1995**, *11*, 1877.
(23) Fajer, J.; Borg, D. C.; Forman, A.; Dolphin, D.; Felton, R. H. *J. Am. Chem. Soc.* **1970**, *92*, 3451.
(24) White, W. I. In *The Porphyrins*; Dolphin, D., Ed.; Academic Press: New York, 1978; Vol. 5; pp 303.
(25) Li, Y.; Liu, L.; He, Z.; Tang, H.; Xiao, S.; Xu, L.; Wang, W. *J. Sol-Gel Sci. Tech.* **2004**, *30*, 29.
(26) Taylor, P. H.; Dellinger, B.; Tirey, D. A. *Int. J. Chem. Kinet.* **1991**, *23*, 1051.
(27) Joo, H.; McKee, M. L. *J. Phys. Chem. A* **2005**, *109*, 3728.
(28) Ishida, S.; Iwamoto, T.; Kabuto, C.; Kira, M. *Chem. Lett.* **2001**, 1102.

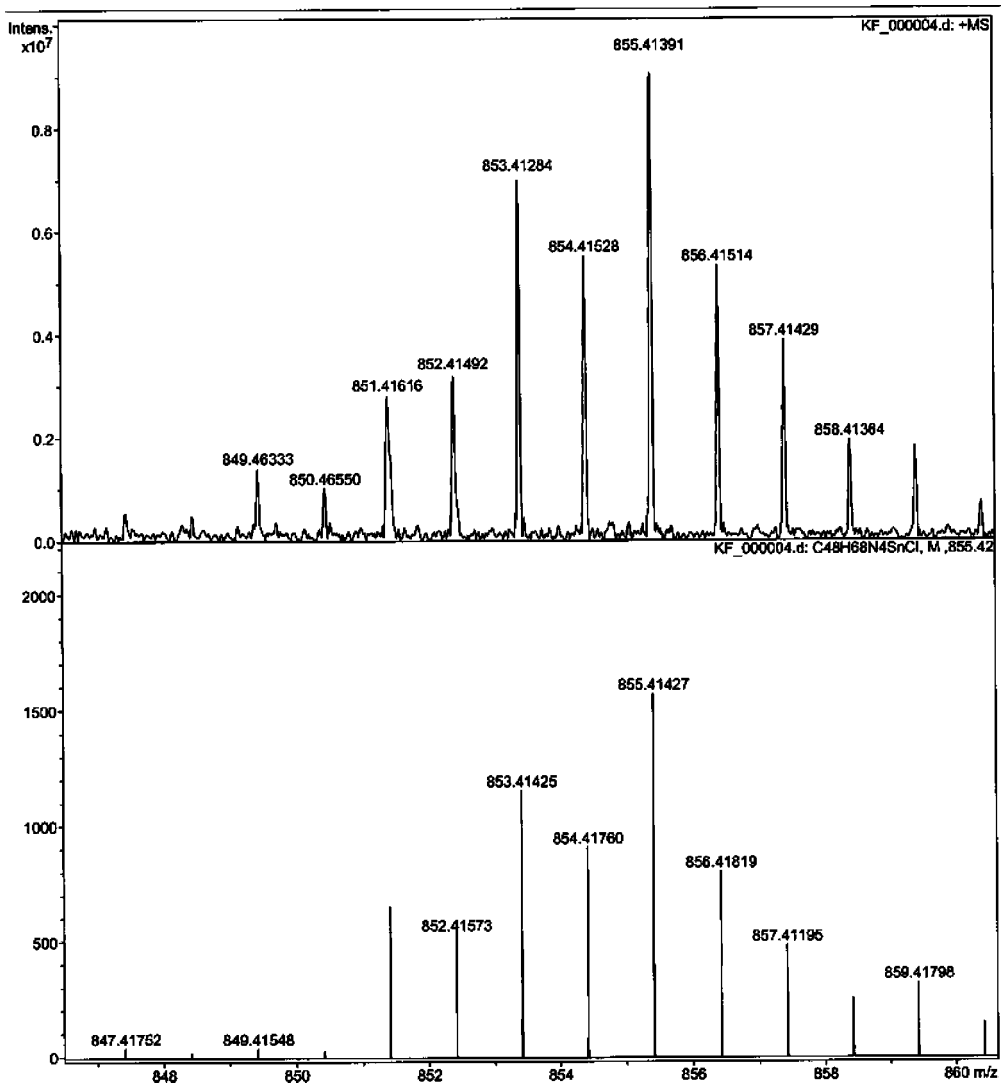

Figure 9. HR−ESI mass spectrum of the dichloro[tetra(heptyl)porphyrinato]tin(IV), and its theoretical required counterpart; ESI−HRMS Found: $[M - Cl]^+$ 855.4139. $C_{48}H_{68}ClN_4Sn$ requires 855.4143.

intense than the CT bands, their identification in the observed spectrum may be difficult.

Experimental Methods

Porphyrin Synthesis. 5,10,15,20-Tetrahepylporphyrin was synthesized as reported previously.[30] Both new compounds were characterized by IR and UV and visible spectroscopy, by MALDI and ESI−HRMS mass spectrometry, ^{1}H NMR and ^{119}Sn NMR spectroscopy and all data were fully consistent with the assigned structures. ^{119}Sn NMR chemical shifts are referenced to external neat $SnMe_4$ taken to be 0 ppm at room temperature. Figures 9 and 10 show the ESI−HRMS mass spectrometry results in agreement with the calculated theoretical profile, also shown.

Synthesis of Dichloro[5,10,15,20-tetra(heptyl)porphyrinato]tin(IV). A solution of 5,10,15,20-tetra(heptyl)porphyrin[30] (0.135 g, 0.192 mmol) and tin(II) dichloride dihydrate (0.830 g, 3.68 mmol) in pyridine (50 mL) was heated at reflux under nitrogen for 1.5 h. The reaction mixture was allowed to cool and poured onto DCM (350 mL). The solution was washed with water (3 × 150 mL) and the organic layer treated with dilute hydrochloric acid (1 M, 1 × 150 mL), then washed with water (1 × 150 mL) again. The organic layers were then dried over anhydrous sodium sulfate and the solvent removed to give a purple-blue solid. Recrystallization of the product from dichloromethane/acetonitrile gave dichloro[5,10,15,20-tetra(heptyl)porphyrinato]tin(IV) as bright purple crystals (0.130 g, 78%), mp > 300 °C. IR ($CHCl_3$) 3034m, 3001m, 1238s, 1204s, 1192m cm^{-1}. UV−vis ($CHCl_3$) 319 (log ε 4.37), 330sh (4.32), 388 (3.87), 408 (4.68), 428 (5.96), 497sh (3.02), 530 (3.55), 562sh (4.11); 571 (4.20), 611 (4.42) nm. UV−vis (DMF) 320 (log ε 4.33), 333sh (4.32), 387 (3.88), 406 (4.68), 426 (5.93), 499sh (3.01), 529 (3.52), 562sh (4.09), 569 (4.24), 609 (4.45) nm. ^{1}H NMR (400 MHz, $CDCl_3$) δ 0.96 (12H, t, J = 7.2 Hz, $C_\eta H_3$); 1.39−1.48 (16H, m, $C_\varepsilon H_2$, $C_\xi H_2$); 1.58−1.65 (8H, m, $C_\delta H_2$); 1.90−1.97 (8H, m, $C_\gamma H_2$); 2.66−2.74 (8H, m, $C_\beta H_2$); 5.11−5.15 (8H, m, $C_\alpha H_2$); 9.82 (8H, s, satellites $^4J_{H-Sn}$ 16.0 Hz, β-pyrrolic H); ^{119}Sn NMR (149 MHz, $CDCl_3$) δ −588.8 (Sn, s). MS (MALDI-TOF) (m/z): 855.5 ($[M - Cl]^+$ requires 855.4). ESI−HRMS Found: $[M - Cl]^+$ 855.4139. $C_{48}H_{68}ClN_4Sn$ requires 855.4143.

Synthesis of Dihydroxo[5,10,15,20-tetra(heptyl)porphyrinato]tin(IV). A solution of the foregoing dichloro[5,10,15,20-tetra(heptyl)porphyrinato]tin(IV) (0.06 g, 0.067 mmol) and anhydrous potassium carbonate (0.373 g, 2.70 mmol) in tetrahydrofuran (50 mL) and water (15 mL) was heated at reflux under nitrogen for 2.5 h. The solution was concentrated in vacuo to remove the tetrahydrofuran and DCM (100 mL) added. The organic layer was washed with water (2 × 100 mL), sodium hydroxide solution (1 M, 2 × 50 mL) then water (2 × 100 mL) again. The organic layer was dried over anhydrous sodium sulfate and the solvent removed

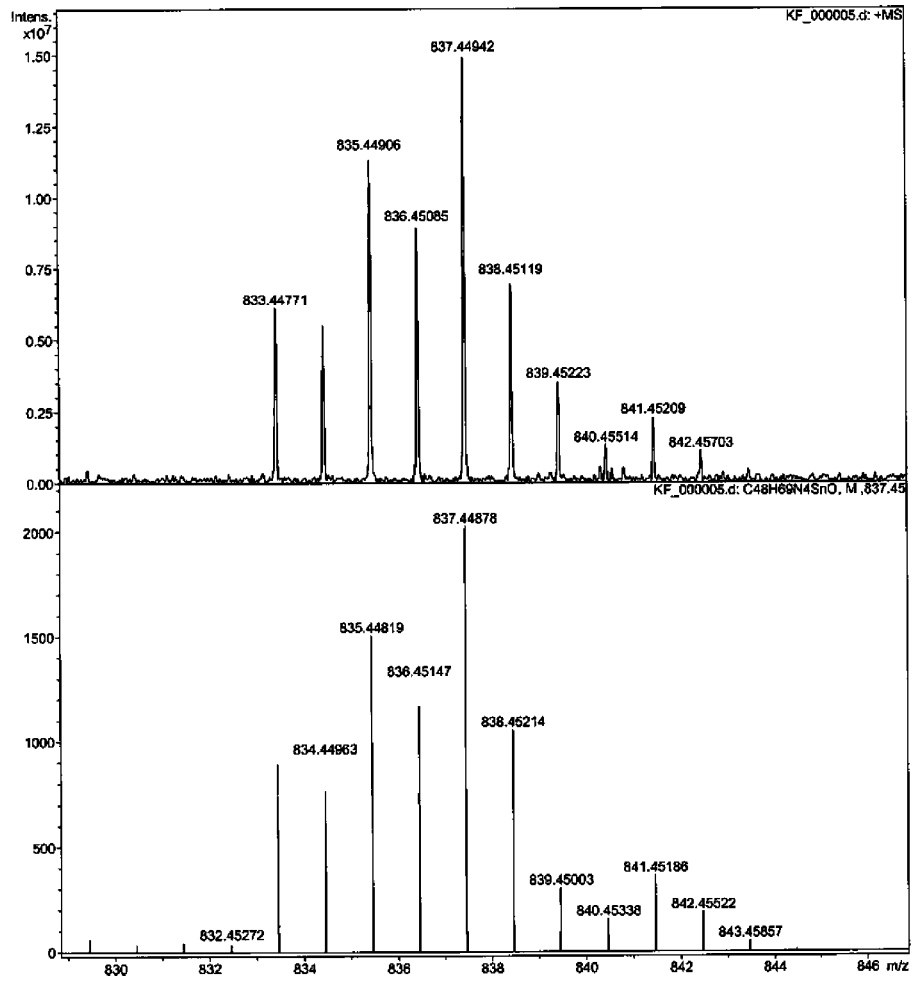

Figure 10. HR−ESI mass spectrum of the dihydroxo[tetra(heptyl)porphyrinato]tin(IV), and its theoretical required counterpart; ESI−HRMS Found: $[M - OH]^+$ 837.4494. $C_{48}H_{69}N_4OSn$ requires 837.4488.

to give dihydroxo[5,10,15,20-tetra(heptyl)porphyrinato]tin(IV) as a purple-blue solid (0.05 g, 92%), mp > 300 °C. IR ($CHCl_3$) 3695w, 3034m, 2959w, 2928w, 2854w, 2361m, 2336m, 1560w, 1261m, 1232m, 1198s, 1095w, 1014w cm^{-1}. UV−vis ($CHCl_3$) 317 (log ϵ 4.11), 404 (4.67), 426 (5.54), 497sh (2.95), 528 (3.34), 569 (4.00), 609 (4.07) nm. ^1H NMR (400 MHz, $CDCl_3$) δ 0.94 (12H, t, J = 7.2 Hz, $C_\eta H_3$); 1.38−1.43 (16H, m, $C_\epsilon H_2$, $C_\xi H_2$); 1.58−1.62 (8H, m, $C_\delta H_2$); 1.89−1.94 (8H, m, $C_\gamma H_2$); 2.16−2.68 (8H, m, $C_\beta H_2$); 5.07−5.11 (8H, m, $C_\alpha H_2$); 9.71 (8H, s, satellites $^4J_{H-Sn}$ 8.0 Hz, β-pyrrolic H); ^{119}Sn NMR (149 MHz, $CDCl_3$) δ −569.0 (Sn, s). MS (ESI) (*m*/*z*): 837.6 ($[M - OH]^+$ requires 837.5). ESI-HRMS Found: $[M - OH]^+$ 837.4494. $C_{48}H_{69}N_4OSn$ requires 837.4488.

In-Fiber Film Fabrication. DMF (bp 153 °C) was redistilled before use and its presence in the fiber monitored using its signature absorption bands in the near-IR at λ = 1200, 1400, and 1600 nm. A pressurization chamber was used to insert the porphyrin/DMF ([dichloro[5,10,15,20-tetra(heptyl)porphyrinato]tin(IV)/DMF] = 1 × 10^{-3} M) solution into the structured fiber sample microchannels (flow rate ≈ 5 cm/min). In order to produce the films, the bulk solution is removed by flushing the holes with purified DMF until no residual porphyrin is detected coming out of the fiber tip. Subsequently, the DMF is removed from the holes by both heating the samples to 50 °C and purging the holes with N_2, leaving only the porphyrin thin-film inside the holes.

In-Fiber Measurements. The optical transmission spectrum through the fiber samples was measured using a 1000 W xenon halogen white light source and an optical spectrum analyzer (OSA). The light was butt-coupled into and out of the PCF fiber ($\Phi_{diameter}$ = 3 μm; lattice pitch $\Lambda \approx$ 3.3 μm, surface roughness: rms <0.5 nm[29]) using standard single mode optical fibers

The films are characterized under two different conditions: (1) in air and without solvent, and (2) with pure solvent inside the holes. The presence of the solvent can be responsible for important physical processes, such as providing free-energy to the molecules to align and/or promote charge-transference. When the solvent is reinserted into the fiber holes, there is an increase in the hole refractive index of 0.4. This leads to an increase in the amount of evanescent field penetrating into the holes. In order to avoid saturation, three different fiber samples are used to investigate different spectral regions with and without solvent. For the dry film case, both the porphyrin Soret and Q bands are characterized using an ∼90 cm long fiber. When the solvent is present, a ∼25 cm long fiber is used to measure the Soret band and a 50 cm length to measure the Q-band.

Film Fabrication and Characterization Inside Cuvette. The porphyrin was dissolved in chloroform at a concentration of 1.6 × 10^{-3} M and added to one face of a horizontally oriented 1-cm UV silica cuvette. The solvent was allowed to evaporate (12 h), leaving a nonuniform film of solid porphyrin. Before deposition, the UV spectrum of the cuvette was recorded and hence the cuvette shown

(29) Canning, J.; Buckley, E.; Huntington, S.; Lyytikäinen, K. *Electrochim. Acta* **2004**, *49*, 3581–3586.
(30) Crossley, M. J.; Thordarson, P.; Bannerman, J. P.; Maynard, P. J. *J. Porphyrins Phthalocyanines* **1998**, *2*, 511.

to be free of absorbate chromophores. All spectroscopic measurements were made on a Varian Cary 4000 UV−vis spectrophotometer.

Film Fabrication and Characterization on Glass Slides. The porphyrin was deposited on glass slides of silica content of ~61.4% and an average surface roughness <10 nm as well as on highly polished high-purity silica slides. The glass slides were chemically cleaned in a MeOH:HCl bath for 30 min and subsequently rinsed with double-distilled water and dried under N_2 flow. A drop-casting technique was used to fabricate the films with 1×10^{-3} M porphyrin solution (same concentration used for the fiber samples) applied on the slide surface and then rinsed with DMF abundantly and left soaking in DMF for 30 min, with subsequent rinsing and dried under N_2. The films on silica slides were constructed analogous to the films inside the cuvettes, using a concentration of 1.6×10^{-3} M, left to evaporate (12 h), washed with DMF, dried with N_2, and finally washed with DCM and dried with N_2 again. High-sensitivity UV measurements performed on the slide before exposure showed no molecular features.

Spectral Fitting. The observed near-IR absorption band was modeled using a Franck−Condon expansion in two vibrational degrees of freedom. One vibration, at $\nu = 1400$ cm^{-1}, was chosen to reflect changes in porphyrin ring modes on oxidation and set to a displacement of 0.8 zero-point units (i.e., a Huang−Rhys factor of 0.64); the other oscillator, at $\nu = 600$ cm^{-1}, was chosen to reflect changes in the Si−O bonds on surface reduction and set at a displacement of 2.2 (i.e., Huang−Rhys factor of 4.84). The other parameters used were an inhomogeneous Gaussian broadening of resolution 650 cm^{-1} and a band-origin frequency of 1.31 eV (945 nm). The depicted band has an average absorption energy (band center, vertical excitation energy) at 1.53 eV (809 nm).

XPS Spectroscopy. The XPS measurements were performed on a Thermo Scientific model ESCALAB220i-XL spectrometer using a monochromated Al Kα (1486.6 eV) line as the X-ray source. The pressure in the measurement chamber during scans was less than 2×10^{-9} millibar. The takeoff angle of the photoelectrons was 90°. Survey scans (0 − 1100 eV binding energy, 100 eV pass energy, 1 eV step size) as well as region scans (20 eV pass energy, 0.1 eV step size) for Sn(3d5), Cl(2p3), C(1s), N(1s) and O1s were recorded. Measurements were obtained from an area of ~1 mm^2.

TD-DFT Calculations. TD-DFT calculations for the optical absorption spectrum of chemisorbed porphyrins were performed using model compounds for the porphyrin and silica surface. For the regular silica surface, $OSi(OSiF_3)_3$ was used for a model,[18] while the tetra-meso alkyl substituents were replaced with hydrogens on the porphyrin; the resulting optimized cluster is shown in Figure 2b. All calculations were performed by Gaussian-03[31] using the B3LYP[32] density functional with the 3−21G basis set[33] for H, C, N, O, and F and the LANL2DZ basis set[34] for Cl, Si, and Sn. Calculations at radical surface defect sites were performed on a structure obtained simply by removing one of the $OSiF_3$ ligands from the central silicon, keeping all other atoms at their previous (silica-lattice-like) positions; the location of the radical center and all spectroscopic properties are somewhat sensitive to the geometrical structure at the central silicon.

Conclusions

Sensitive, broadband, long-path-length evanescent field spectroscopy (EFS) is introduced to the study of chemisorption and is used to demonstrate that thin films of organic materials (porphyrins) adhered to the walls of photonic crystal fiber channels have a range of novel optical properties. A dichlorotin(IV) porphyrin was used and the experimental results are consistent with a chemisorbed layer produced by reaction with a surface silanol to generate a surface Si−O−Sn linkage. Overall, EFS is a powerful wide band spectroscopic tool by which thin films on fused silica can be investigated with very high sensitivity. It is shown to be particularly relevant to the characterization of the silica surface inside the channels of structured optical fibers, and allows for high sensitivity as the length of the fiber may be varied over a very wide range. This silica surface has properties that are significantly altered from those of other silica surfaces as a result of the mechanical deformation and drying and quenching processes that create the fibers but until now has been poorly characterized. In particular, the novel spectroscopic effects that are observed in this work are interpreted as arising from the adsorbate molecules binding to mechanical-strain induced surface defect sites on the silica. In general, as well as providing a very sensitive molecular detector by making use of the fiber holes to support gas and liquid flows and to access propagating modes, it also allows for new photonic and electronic hybrid technologies with applications bringing together electronic, photovoltaic and photonic properties of porphyrin systems that lay the foundation for optical circuitry.[35]

Acknowledgment. C. Martelli is supported by CAPES-Brazil. Australian Research Council Discovery Project grants (DP0450601 & DP0770692 to J.C., and DP0773847 to M.J.C. and J.R.R.) funded this work. The optical fiber was fabricated by K. Digweed, B. Ashton, M. Stevenson, and J. Digweed.

Supporting Information Available: Complete ref 31. General background material for structured optical fibers such as photonic crystal fibers can be found in refs 4 and 36. This material is available free of charge via the Internet at http://pubs.acs.org.

JA8081473

(31) Frisch, M. J.; et al. *GAUSSIAN 03 Rev. B2*; Gaussian Inc.: Pitsburgh, PA, 2003.
(32) Becke, A. D. *J. Chem. Phys.* **1993**, *98*, 5648.
(33) Binkley, J. S.; Pople, J. A.; Hehre, W. J. *J. Am. Chem. Soc.* **1980**, *102*, 939.
(34) Hay, P. J.; Wadt, W. R. *J. Chem. Phys.* **1985**, *82*, 270.
(35) Jacobsen, R. S.; Andersen, K. N.; Borel, P. I.; Fage-Pedersen, J.; Frandsen, L. H.; Hansen, O.; Kristensen, M.; Lavrinenko, A. V.; Moulin, G.; Peucheret, C.; Zsigri, B.; Bjarklev, A. *Nature* **2006**, *41*, 199.
(36) Canning J., In *Frontiers in Lasers and Electro-Optics Research*; Arkin, W. T., Ed.; Nova Science Publishers, United States, 2006, Chapter *1*, pp 1−63.